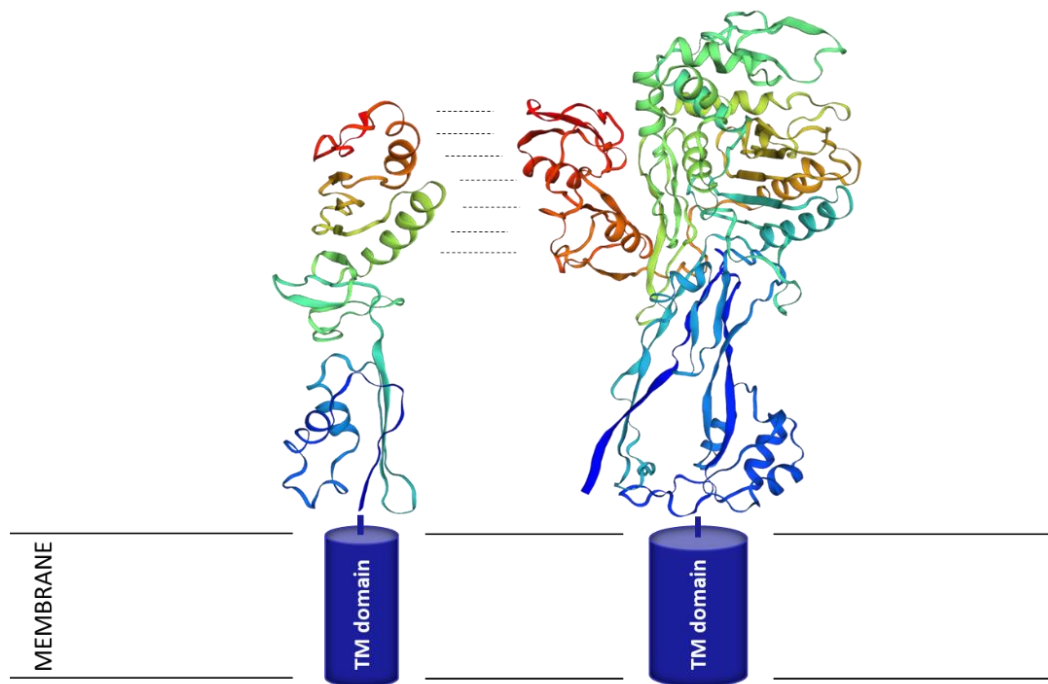




Master Project:

Interaction between PBP2b and DivIB in *Bacillus subtilis*



Alicia Maciá Valero – S3264742

Supervisor: Dr. Dirk-Jan Scheffers

Molecular Microbiology Department

February – July 2019

Abstract

The cell wall is an essential component for bacterial cells, which provides them with shape, integrity, protection from the environment and osmotic pressure shocks, and a scaffold for anchoring of other proteins. Synthesis of the main component, peptidoglycan, is mediated by a complex of different proteins during cell division and elongation. One of those proteins, PBP2b, essential in *Bacillus subtilis*, is recruited to the division site by DivIB in order to perform the transpeptidase activity responsible for cross-linking of peptidoglycan. The interaction between DivIB and PBP2b has been demonstrated in the past. However, details about that interaction such as the orientation or residues involved are yet to be deciphered. PBP2b contains two PASTA domains in the sequence whose function is hitherto unknown. In this work, it is demonstrated by co-immunoprecipitation assays and observation under the microscope that deletion of PBP2b PASTA domains negatively affects the DivIB-PBP2b interaction. Together with previous bacterial two hybrid experiments from the group, these results suggest that, although not exclusively, PASTA domains from PBP2b are involved in the DivIB-PBP2b interaction and most likely stabilize it, improving the efficiency of PBP2b recruitment to the division site during cell wall biosynthesis.

Keywords: *Bacillus subtilis*, cell wall, divisome, PBP2b, DivIB, PASTA domain, protein-protein interaction, co-immunoprecipitation, fluorescence microscopy.

Abbreviations

B. subtilis: *Bacillus subtilis*

Cryo-TEM: cryo- Transmission Electron Microscopy

DDM: *n*-dodecyl- β -D-maltopyranoside

DNA: Deoxyribonucleic acid

E. coli: *Escherichia coli*

GFP: Green Fluorescence Protein

LB: Lysogeny Broth

m-DAP: *meso*-diaminopimelic acid

NAG: N-acetyl-glucosamine (also GlcNAc)

NAM: N-acetyl-muramic acid (also MurNAc)

PBP: Penicillin-Binding Protein

PBS: Phosphate-Buffered Saline

PASTA: Penicillin-Binding Protein and Serine/Threonine Kinase Associated

PCR: Polymerase Chain Reaction

PG: Peptidoglycan

PVDF: Polyvinylidene difluoride

S. pneumoniae: *Streptococcus pneumoniae*

SDS-PAGE: Sodium dodecyl sulfate – Polyacrylamide gel electrophoresis

STPK: Serine and Threonine protein kinase

TAE: Tris-base, acetic acid and EDTA buffer

TBE: Tris-base, borate and EDTA buffer

TBST: Tris buffer saline with Tween 20

Table of contents

1. Introduction	5
1.1 Composition and structure of the cell wall in <i>B. subtilis</i>	5
1.2 Synthesis of peptidoglycan during cell division	5
1.3 Penicillin Binding Proteins: the essential PBP2b and its interaction with DivIB	6
1.4 Influence of PBP2b PASTA domains in the interaction with DivIB.....	7
2. Materials and methods	9
2.1 Bacterial strains, characteristics and growth conditions	9
2.2 Co-immunoprecipitation.....	9
2.3 SDS-PAGE and immunoblotting	10
2.4 Fluorescence microscopy	10
2.5 Construction of PASTA mutants	11
3. Results.....	13
Deletion of PASTA domains has a negative effect on DivIB-PBP2b interaction	13
PBPs localisation at the division site is hindered in the absence of PASTA domains	16
Cloning of PASTA constructs.....	17
4. Discussion and conclusions.....	17
5. Further work.....	20
6. References.....	20

1. Introduction

1.1 Composition and structure of the cell wall in *B. subtilis*

The cell wall is a protective layer that surrounds the cells of most of bacterial species including *Bacillus subtilis*, with some exceptions such as the division Tenericutes¹. This envelope provides bacteria with shape, structural support and integrity but also protection from the environment (as cell wall constitutes the first contact with it in the case of Gram-positive bacteria), maintenance of osmotic pressure and a scaffold for the anchoring of proteins involved in certain interactions, amongst other functions^{2,3}. As might be expected, certain modifications, degradation or inhibition of its synthesis, due to either external factors or mutations, leads cells to lysis or non-viability⁴. Therefore, this structural component has been one of the main targets for development of antimicrobial compounds among the years⁵.

Based on cryo-TEM results, the *B. subtilis* cell wall can be divided in three sections: an inner wall zone, an area suggested to be the Gram-positive equivalent of the periplasm and an outer wall zone⁶. As stated before, in contrast with Gram-negative bacteria, Gram-positive bacteria lack an outer membrane; thus, the external milieu is in direct contact with the cell wall. Consequently, the cell wall is thicker and contains, for that species, 10 to 30 layers of PG strands. *B. subtilis*, for instance, shows considerably large strands compared to other species, of at least 500 disaccharide units⁷.

The main component of bacterial cell walls is peptidoglycan (PG), although other proteins and essential compounds as teichuronic and teichoic acid polymers can be found attached^{8,9}. Peptidoglycan, also called murein, is a polymer of parallel glycan strands, whose basic units are alternating N-acetyl-glucosamine (NAG) and N-acetyl-muramic acid (NAM) residues linked by a β -(1, 4) glycosidic bond (Figure 1a). The latter monosaccharide contains a short peptidic chain, usually a pentapeptide, which is responsible for the cross-linking between neighbouring strands. In *B. subtilis*, the sequence for NAM pentapeptides is L-Ala₍₁₎ – D-Glu₍₂₎ – *m*-DAP₍₃₎ – D-Ala₍₄₎ – D-Ala₍₅₎ and the cross-bridge occurs between an *m*-DAP₍₃₎ as acceptor and a D-Ala₍₄₎ from another chain as a donor, resulting in a 3-4 crosslink and the consequent release of the terminal D-Ala₍₅₎ from the second oligopeptide^{10,11}. This reaction takes place during PG synthesis, which occurs during cell division and elongation. In the following section, biosynthesis will be further explained focusing on cell division and proteins involved in the process.

1.2 Synthesis of peptidoglycan during cell division

Cell division is understood as the process by which a cell divides into two new individual ones; in the case of most prokaryotes, by binary fission. For this purpose, cells form a septum and synthesise membrane molecules but also cell wall components, which leads to some local differences in terms of structure and composition among the cell¹². Precursors of such components are synthesised in the cytosol^{13–15}. In short, UDP-NAM-pentapeptide is produced by several enzymes encoded by *mur* genes. Then, the membrane-associated enzyme *MraY* ligates that molecule to an undecaprenyl (C₅₅) carrier lipid for the subsequent *flipping* across the membrane, getting lipid I as a product. Subsequently, *MurG* catalyses the ligation of lipid I to a NAG residue, producing the disaccharide called lipid II¹⁶ and concluding the cytoplasmic steps. A flippase translocates lipid II to the other side of the cytoplasmic membrane, where the final steps of PG assembly take place. Then, lipid II is incorporated into PG strands (transglycosylation) and the lipid carrier is released as C55-isoprenyl-pyrophosphate and

recycled into the cytoplasm to act again as a substrate for *MraY*. The growing glycan chains are covalently linked via peptide bond cross-links between pentapeptides of NAM residues from different strands as explained in the previous section (transpeptidation)¹⁷. As stated before, the terminal D-Ala₍₅₎ from the donor stem peptide is released during transpeptidation. D-Ala₍₄₎ – D-Ala₍₅₎ residues from the acceptor pentapeptide are also removed in a reaction referred to as carboxypeptidation, although this may occur before the cross-linking takes place as well. The set of reactions that constitute non-cytosolic PG synthesis steps is displayed in Figure 1b and is mediated mainly by a group of proteins called Penicillin-Binding Proteins (PBPs) that will be described below. However, other proteins are suggested to be involved¹⁸ in the process, like *RodA*, which has already been reported to show transglycosylase activity in *B. subtilis*¹⁹.

The cell wall is synthesised during cell division and elongation, but also continuously hydrolysed catalysed by certain proteins known as autolysins. Hydrolysis is tightly controlled. It has been observed in *B. subtilis* that the resulting muropeptides from PG decomposition are further processed to NAG and NAM residues, transported back into the cytoplasm and reused in PG synthesis, showing, for the first time in Gram-positive bacteria, recycling of cell wall components²⁰. Moreover, genes homologous to Gram-negative cell wall recovery genes have been reported in this organism²¹.

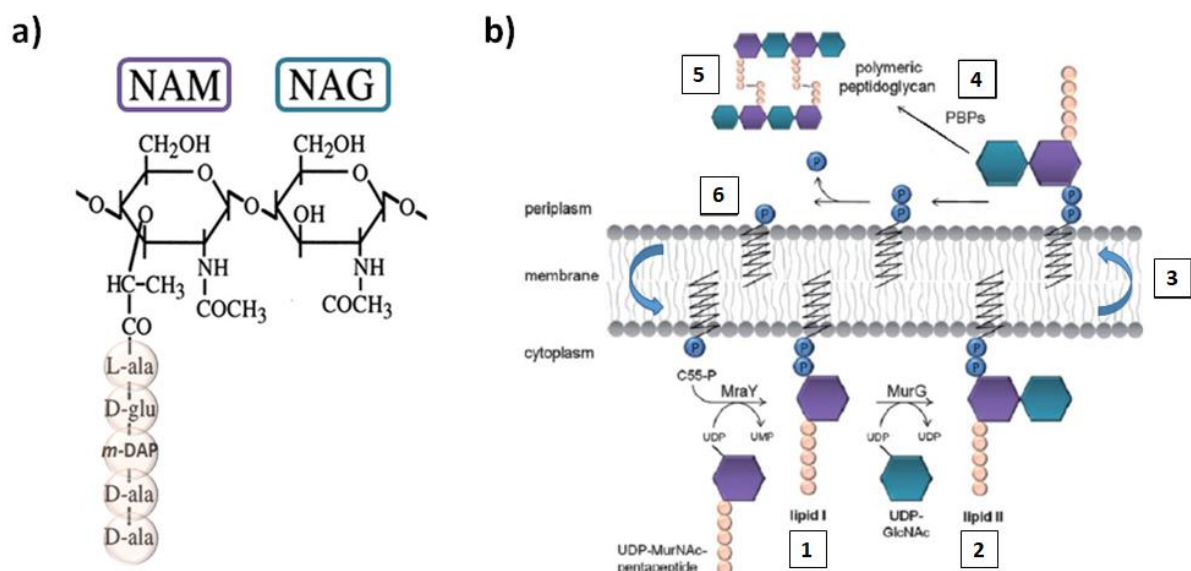


Figure 1. a) Chemical structure of peptidoglycan disaccharide subunits N-acetyl-glucosamine (NAG or GlcNAc) and N-acetylmuramic acid (NAM or MurNAc) linked by a β -(1, 4) glycosidic bond. b) Schematic representation of peptidoglycan biosynthesis. Adapted from M. Wilmes *et al.* (2011)²². 1: synthesis of lipid I; 2: synthesis of lipid II; 3: translocation or *flipping* of lipid II across the membrane; 4: transglycosylation; 5: transpeptidation between a *m*-DAP₍₃₎ acceptor and a D-Ala₍₄₎ donor of two NAM molecules with the consequent release of terminal D-Ala₍₅₎ from donor pentapeptide and carboxypeptidation of the terminal D-Ala₍₄₎-D-Ala₍₅₎ molecules from the acceptor chain; 6: carrier lipid recycling.

1.3 Penicillin Binding Proteins: the essential PBP2b and its interaction with DivIB

Penicillin Binding Proteins are enzymes responsible for most of the reactions that take place during PG biosynthesis. Those proteins bind and show affinity for β -lactam rings, therefore have been used over the years as target for different antibiotics such as penicillin²³. However, some have suffered point mutations that allow them to hydrolyse those rings, leading to the well-known alarming antibiotic resistance^{24–26}. Depending on the size, PBPs can be classified in low molecular mass (LMM) and high molecular mass (HMM)²⁷. Some LMM PBPs have carboxypeptidation activity, which means, cleave the

two terminal alanine residues of acceptor stem peptides. PBP5 is the major carboxypeptidase in *B. subtilis*²⁸. Other LMM PBPs work as endopeptidases. Those proteins, such as PbpX²⁹, mediate the inverse reaction to transpeptidation. Consequentially, cross-links are cleaved and the PG strands are allowed to expand. According to the structure and catalytic activity, HMM PBPs are likewise subdivided in two different categories: class A and class B. Class A PBPs, also known as bi-functional, present transglycosylase activity at the N-terminal domain and transpeptidase activity at the C-terminal domain. A representative example from this group is PBP1³⁰. Finally, class B PBPs contain a C-terminal domain with transpeptidase activity. The main subject of this work and also a member of this class is PBP2b. PBP2b is the only essential PBP in *B. subtilis*, as mutants form filamentous cells and eventually lyse^{31,32}. Nevertheless, it has been reported that inactivation of the transpeptidase activity does not affect cells phenotype or viability^{12,33}; thus, the essentiality of this enzyme does not lie in that function. PBP2b is found both in vegetative cells and spores³¹ as part of the late divisome³⁴. During cell division, PBP2b is located at the division site, where it has been localised by different fluorescence microscopy experiments^{32,35}. PBP2b interacts with DivIB, co-localised at the division site together with FtsL and DivIC³⁴. The interaction between those two proteins has been already proven by bacterial two hybrid assay³⁶ and artificial septal targeting³⁷. However, there is not much information about the amino acids involved, nor the orientation of both molecules. Heterologous septal targeting results of DivIB mutants show that residues 229 to 257 from β -domain are critical for the interaction with PBP2b and that the γ -domain might regulate it negatively³⁸. Molecular modelling of both proteins suggests that the extracytoplasmic region of PBP2b must be the major site of the interaction³⁸. In this work, it will be explored whether the C-terminal domain of PBP2b is involved in the interaction with DivIB.

1.4 Influence of PBP2b PASTA domains in the interaction with DivIB

PBP2b sequence is structured with a cytoplasmic domain, a transmembrane domain, a dimerization domain implicated in PBP polymerization, a transpeptidase domain responsible for the crosslinking during PG synthesis and two PASTA domains. PASTA domains are short peptidic sequences (65 – 70 aa) found at the C-terminal of PBPs and Serine and Threonine protein kinases (STPKs), which are enzymes that signal for bacterial growth, virulence and reactivation from dormancy by regulating protein phosphorylation^{39,40}. PASTA domains were initially observed in *Streptococcus pneumoniae*⁴¹ and subsequently so termed for penicillin-binding protein and serine/threonine kinase associated domain⁴². Proteins of Gram-positive bacteria and Mycobacteria have PASTA domains, remarkably in *Bacillus* and *Clostridium* genera. Although sequence alignment of those domains shows a low homology (below 10 %)⁴², their structure seems to be strongly conserved, with a typical fold consisting of an N-terminal α -helix packed against three antiparallel β -sheet strands, where the first and second strands are linked by a loop (Figure 2). PASTA domains are frequently present in multiple copies in a single protein. In the case of PBPs, proteins have been seen to have between one and three of those domains. In contrast, STPKs are known to contain multiple copies up to a maximum of six domains⁴³.

The function of PASTA domains is yet to be deciphered. In *B. subtilis*, there are three proteins that have PASTA domains: one STPK, PrkC; and two PBPs, SpoVD and PBP2b. PrkC induces germination of bacterial spores in response to DAP-muropeptides and it has been verified that PASTA domains of this enzyme function as PG-binders⁴⁴, as the deletion of those regions inhibits that process^{45,46}. SpoVD mediates the synthesis of spore peptidoglycan⁴⁷. By contrast, the function of SpoVD PASTA domain is still unknown. E. Bukowska-Faniband and L. Hederstedt ruled out the possibility of a catalytic activity

of the transpeptidase domain or a role linked to protein localisation⁴⁸ and their statements were confirmed when N-terminal of SpoVD was reported to determine the forespore targeting of the protein⁴⁹. In line with those results, they suggested an influence in protein stability and binding efficiency of the substrate to the active site of the transpeptidase domain. Finally, PBP2b PASTA domains function remains enigmatic.

PrkC is not the only protein that shows peptidoglycan binding at the C-terminal PASTA domains. PknB PASTA domains from *Mycobacterium tuberculosis* recognise expanding PG strands and regulate production of PBPs for cell wall integrity and bacterial growth^{50,51}. *Staphylococcus aureus* Stk1 also presents three PASTA domains that, based on crystal structure and molecular modelling, are likely to interact with the cell wall PG residues⁵². StkP from *S. pneumoniae* binds to uncross-linked peptidoglycan and participates in cell wall synthesis regulation^{53,54}. Interestingly, all proteins that bind to PG show a conserved region with an Arg or Glu residue (Figure 2). Indeed, mutation of Arg500 from PrkC has been shown to suppress binding to peptidoglycan⁴⁴. Conversely, other PASTA proteins that are known to not be PG-binders contain a Pro in that position⁵⁵; consequently, the PBP2b PASTA domains are likely to have another function rather than PG binding, as there is a proline residue in that location. Deletion of PBP2b PASTA domains has been previously reported to have no effects in terms of growth rate neither is essential for localization of the protein at the division site¹². On the other hand, the involvement in cell division cannot be discarded, as cells without those two regions show an elongated phenotype that gets more acute at higher temperatures⁵⁶. Bacterial two hybrid assays showed that PASTA domains are not required for DivIB-PBP2b interaction, although the deletion has a negative effect according to β -galactosidase activity results⁵⁶. Similarly to SpoVD, it could be that, although not exclusively, PBP2b PASTA domains are involved in the interaction between those divisome proteins to a yet uncertain extent.

In this work, the effect of PBP2b PASTA domains deletion on the interaction with DivIB during cell division will be explored. With that aim in view, co-immunoprecipitation analysis and the subsequent quantification of results with full length protein and a truncated version of PBP2b (without PASTA domains) will be performed. Investigation of alterations in cell localisation pattern of PBP2b will constitute another approach of the study about the influence of PASTA domains in DivIB-PBP2b interaction. Finally, constructs with one single domain will be cloned in order to obtain further information.

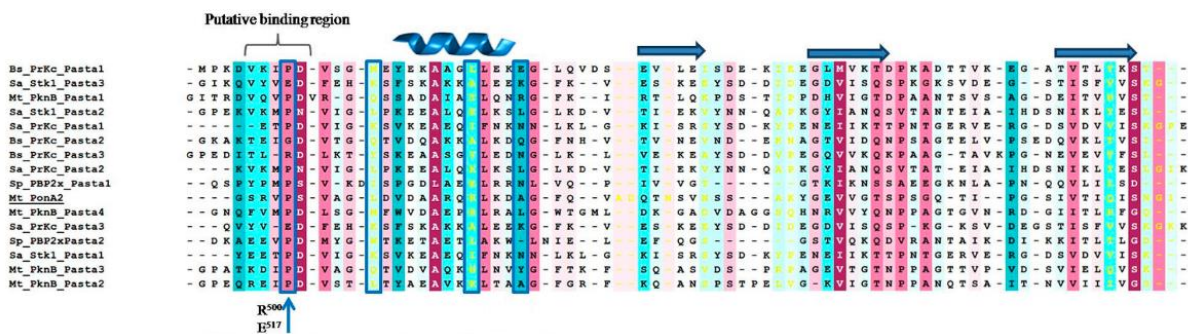


Figure 2. Edited from L. Calvanese *et al.* (2016)⁵⁵. Sequence alignment of different PASTA domains. Conserved amino acids are coloured in magenta, residues of average conservation are white and variable amino acids are turquoise. A ribbon representation of secondary structure is shown on top of the sequences. Putative binding region is highlighted and arrow corresponds to Arg/Glu or Pro residue depending on the ability to bind peptidoglycan.

2. Materials and methods

2.1 Bacterial strains, characteristics and growth conditions

Strains used in this work are listed in Table 1. *E. coli* and *B. subtilis* strains were incubated in LB broth medium at 37°C and 30°C, respectively. Spectinomycin (100 µg/mL) and erythromycin (1 µg/mL) were added as a selective marker when required. In order to induce *pbpB* expression under P_{xyl} promoter control, 0.2% (wt/vol) xylose was used unless otherwise stated.

Name	Characteristics	Source
STRAINS		
4132	<i>trpC2 chr::P_{spac}-pbpB neo amyE::pDMA001(spc P_{xyl}-gfpmut-pbpB)</i>	D. M. Angeles <i>et. al.</i> , 2017 ¹²
4133	<i>trpC2 chr::P_{spac}-pbpB neo amyE::pDMA002(spc P_{xyl}-gfpmut-pbpB¹⁻¹⁹⁹¹)</i>	D. M. Angeles <i>et. al.</i> , 2017 ¹²
4174	<i>divIB-3xFLAG ermC amyE::pDMA001(spc P_{xyl}-gfpmut-pbpB)</i>	Laboratory collection
4175	<i>divIB-3xFLAG ermC amyE::pDMA002(spc P_{xyl}-gfpmut-pbpB¹⁻¹⁹⁹¹)</i>	Laboratory collection
GP2005	<i>divIB-3xFLAG ermC</i>	Gift from Jörg Stülke
DH5α	<i>F- endA1 glnV44 thi-1 recA1 relA1 gyrA96 deoR nupG purB20 φ80d-lacZΔM15 Δ(lacZYA-argF) U169, hsdR17(rK-mK+), λ-</i>	Laboratory collection
4177	<i>DH5α pDMA001(spc P_{xyl}-gfpmut-pbpB)</i>	This work
4178	<i>DH5α pDMA002(spc P_{xyl}-gfpmut-pbpB¹⁻¹⁹⁹¹)</i>	This work
PLASMIDS		
pDMA001	<i>bla amyE3' spc P_{xyl}- gfpmut-pbpB amyE5'</i>	D. M. Angeles <i>et. al.</i> , 2017 ¹²
pDMA002	<i>bla amyE3' spc P_{xyl}-gfpmut-pbpB¹⁻¹⁹⁹¹ amyE5'</i>	D. M. Angeles <i>et. al.</i> , 2017 ¹²
pAMV01	<i>bla amyE3' spc P_{xyl}-gfpmut-pbpB^{PASTA1} amyE5'</i>	This work
pAMV02	<i>bla amyE3' spc P_{xyl}-gfpmut-pbpB^{PASTA2} amyE5'</i>	This work

Table 1. Strains used in this work.

2.2 Co-immunoprecipitation

Strains GP2005, 4174 and 4175 were grown overnight in presence of the corresponding antibiotic. For protein production, cultures were diluted 1:100 and induced with 0.2% (wt/vol) until OD₆₀₀ ≈ 0.4. Some steps of this protocol were adapted from D.J. Scheffers *et. al* (2007)⁵⁷. Cells were harvested for 10 min at 8.000 x g at 4°C, resuspended in buffer I (10mM Tris-HCl, 150mM NaCl, pH 7.4 with cComplete™ ULTRA Tablets Mini EDTA-free, EASYpack protease inhibitors (Sigma-Aldrich)) and disrupted via sonication. Cell debris were discarded and membranes were isolated through ultracentrifugation at 100.000 x g for 1 h at 4°C and solubilised in 1% (wt/vol) *n*-dodecyl-β-D-maltopyranoside (DDM; Anatrace) buffer I by gentle shaking at 4°C on a roller mx for 30 min. Insoluble fraction was separated by the use of a second ultracentrifugation step at same conditions for 30 min.

Protein concentration was determined using DC™ (detergent compatible) protein assay kit (Bio-Rad Laboratories) and 200 ng total membrane protein were incubated for 1 h at 4°C with gentle shaking on a roller mix with i) 25 µl GFP-Trap® agarose beads (Chromotek) or ii) 40 µl anti-flag M2 Affinity agarose beads (Sigma-Aldrich) in a final volume of 100 µl 1% (wt/vol) DDM buffer I or buffer II (as buffer I, but with 50mM Tris-HCl), respectively, according to manufacturers' recommendations. Beads had been previously blocked by 1 h incubation at the same conditions with 1% (wt/vol) BSA in the corresponding buffer. After incubation, flowthrough was collected (100 µl) using centrifugation (2.500 x g for 2 min with GFP-Trap® beads and 8.200 x g for 30 s with anti-flag beads) at 4°C and beads were washed twice (three times in the case of anti-flag beads) and resuspended in 40 µl of 1xSDS-PAGE sample buffer. Low-binding tubes (Thermo Fisher Scientific) were used during the whole process.

2.3 SDS-PAGE and immunoblotting

5 µl input, 5 µl flowthrough and 14 µl eluate fractions were loaded in 10% (vol/vol) acrylamide gels for SDS-PAGE for all three strains and run for 20 min at 80 V and for 90 min at 120 V. In order to roughly estimate protein purity and concentration, some gels were run in duplicates and stained with Silver Staining due to its higher sensitivity⁵⁸. For silver staining, gels were fixed with 50% (vol/vol) ethanol, 12% (vol/vol) acetic acid and 0.037% (wt/vol) formaldehyde, washed in 50% (vol/vol) ethanol, sensitized for 1 min with 0.02% (wt/vol) Na₂S₂O₃ and stained for 30 min in a cold 0.2% (wt/vol) AgNO₃ and 0.037% (wt/vol) formaldehyde solution. Development was carried out in 6% (wt/vol) Na₂CO₃, 2% (vol/vol) sensitizer solution and 0.019% (wt/vol) formaldehyde and stopped with 50% (vol/vol) methanol and 12% (vol/vol) acetic acid.

Duplicate gels were transferred to PVDF membranes by wet Western Blot transfer in 25 mM Tris-HCl pH?, 192 mM glycine, 15% (vol/vol) methanol at 55 V for 2 h. Membranes were blocked overnight at 4°C in 1% (wt/vol) skim milk (Oxoid) and incubated for 1h with i) anti-flag M2 mouse monoclonal (1:1000) from Sigma-Aldrich, ii) anti-GFP pAb rabbit polyclonal (1:1000) from Chromotek or iii) both on a rocking platform and, subsequently, incubated for 1h with the corresponding secondary antibody: anti-mouse (1:10000) and/or anti-rabbit (1:10000), both from Sigma-Aldrich. Antibodies were diluted in TBST (50 mM Tris 150 mM NaCl 0.05% (vol/vol) Tween 20 pH 7.6), also used as wash solution. Blots were developed with CDP-Star (Roche) and chemiluminescence was detected using a Fujifilm LAS4000 luminescence imager and the Image Reader LAS 4000 Software (GE Healthcare Life Science). Images were analysed using the software Image J(rsb.info.nih.gov/ij/)⁵⁹.

2.4 Fluorescence microscopy

Strains 4132 and 4133 were grown overnight in LB with 0.2% (wt/vol) xylose and spectinomycin. Cultures were diluted 1:100 and induced with 0.5% xylose (wt/vol) until OD₆₀₀ ≈ 0.4. Live cells were resuspended in 50 µL of PBS (137 mM NaCl; 2.7 mM KCl; 10 mM Na₂HPO₄; 1.8 mM KH₂PO₄, pH 7.4), spotted on 1 % (wt/vol) agarose pads and imaged using a Nikon Ti-E microscope (Nikon Instruments, Tokyo, Japan) equipped with a Hamamatsu Orca Flash4.0 camera. Images were analysed using the software Image J⁵⁹ (rsb.info.nih.gov/ij/). For cell counting, Cell Counter tool was used and results were assessed through a Chi-Square test⁶⁰ performed with <https://www.socscistatistics.com/tests/chisquare/> (accessed July 5th, 2019). For fluorescence intensity measurements, ChainTracer⁶¹ and SeptaMarker, plugins from the macro tool ObjectJ

(sils.fnwi.uva.nl/bcb/objectj/), were used. The first removed the background of pictures taken for a proper observation. The latter quantified fluorescence intensity in arbitrary units according to the following equation: $I = I_s - \frac{I_L + I_R}{2}$, where I_s represents intensity in the septum and I_R and I_L correspond to the fluorescence background given by the cytosol (Figure 3). A boxplot representation and a t-test statistical analysis⁶² of the results were performed using IBM SPSS Statistics Version 24 (International Business Machines Corporation, New York, USA).

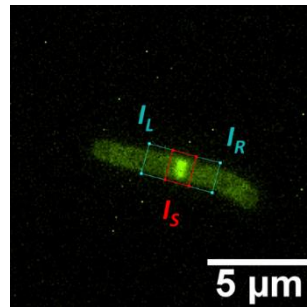


Figure 3. Schematic visualisation of fluorescence intensity measurement with plugin SeptaMarker.

2.5 Construction of PASTA mutants

For molecular cloning, pDMA001 and pDMA002 were required as templates. Therefore, plasmids were previously transformed in *E. coli* DH5 α via heat-shock transformation⁶³. Transformants were checked by colony PCR using primers dma043 and dma044. Consequently, plasmid isolation was performed using a GenElute™ Plasmid Miniprep Kit (Sigma-Aldrich).

PASTA mutants construction was planned based on restriction free cloning⁶⁴. Primers used are listed in Table 2 and were designed using <http://www.rf-cloning.org/> (accessed July 5th, 2019) and checked using the software package Clone Manager Basic 9 (scied.com/pr_cmbas.htm). Primers amv01 and amv02 introduced a stop codon in pDMA001 after PASTA1 and made a deletion of PASTA2 after two consecutive PCRs. The first PCR generated two fragments that correspond to the flanking regions of the domain to be deleted and were used as mega-primers in a second PCR. The second polymerase reaction introduced PASTA1 into pDMA002, resulting in pAMV01. The same procedure was followed with primers amv03 and amv04 in order to produce a deletion of PASTA1, getting as a result pAMV02 (Figure 4). Phusion® High-Fidelity PCR Master Mix (Thermo Fisher Scientific) was used for all PCR reactions under the conditions stated in Table 2. For the visualisation of results, mega-primers were run in 2% (wt/vol) agarose TBE gels and second PCR products were observed in 1% (wt/vol) agarose TAE gels, following standard conditions for DNA agarose gel electrophoresis⁶⁵.

Primer	Sequence 5' → 3'	PCR conditions
amv01 (Trans-PASTA1-fw)	ACCAACTGAAAAATCTGACTCAGATAAGGAAGAA ACAAAAGCGCAGACAATGC	<u>1st PCR</u> : 1x 98 °C 1min, 30x (98°C 10s, 58°C 20s, 72°C 15s), 1x 72°C 5min <u>2nd PCR</u> : 1x 98 °C 1min, 20x (98°C 10s, 55°C 20s, 72°C 15s), 1x 72°C 5min
amv02 (PASTA1-stop-rv)	GGGGGGGCCCGTGGATCCG TTAGCCGCCCGTTTT CAGGAA	
amv03 (Trans-PASTA2-fw)	ACCAACTGAAAAATCTGACTCAGATAAGGAAGAA AAAATCAAATGCCTGATATGACAG	<u>1st PCR</u> : 1x 98 °C 1min, 30x (98°C 10s, 60°C 20s, 72°C 15s), 1x 72°C 5min <u>2nd PCR</u> : 1x 98 °C 1min, 20x (98°C 10s, 55°C 20s, 72°C 15s), 1x 72°C 5min
amv04 (PASTA2-stop-rv)	GGGGGGGCCCGTGGATCCG TTATTAATCAGGATT TTTAAACTTAACC	
dma043 (amyE-rv)	CCGAGTCATTATATAAACCATTTAGCACGTAAT	<u>Colony PCR</u> : 1x 98 °C 30s, 30x (98°C 5s, 55°C 1min, 72°C 15s), 1x 72°C 1min
dma044 (spec-fw)	CTAATCAAATAGTGAGGAGGATATATTTG	

Table 2. Primers used in this work. Description of the primers in brackets. Bold nucleotides correspond to PASTA domains sequence. Red nucleotides correspond to stop codon.

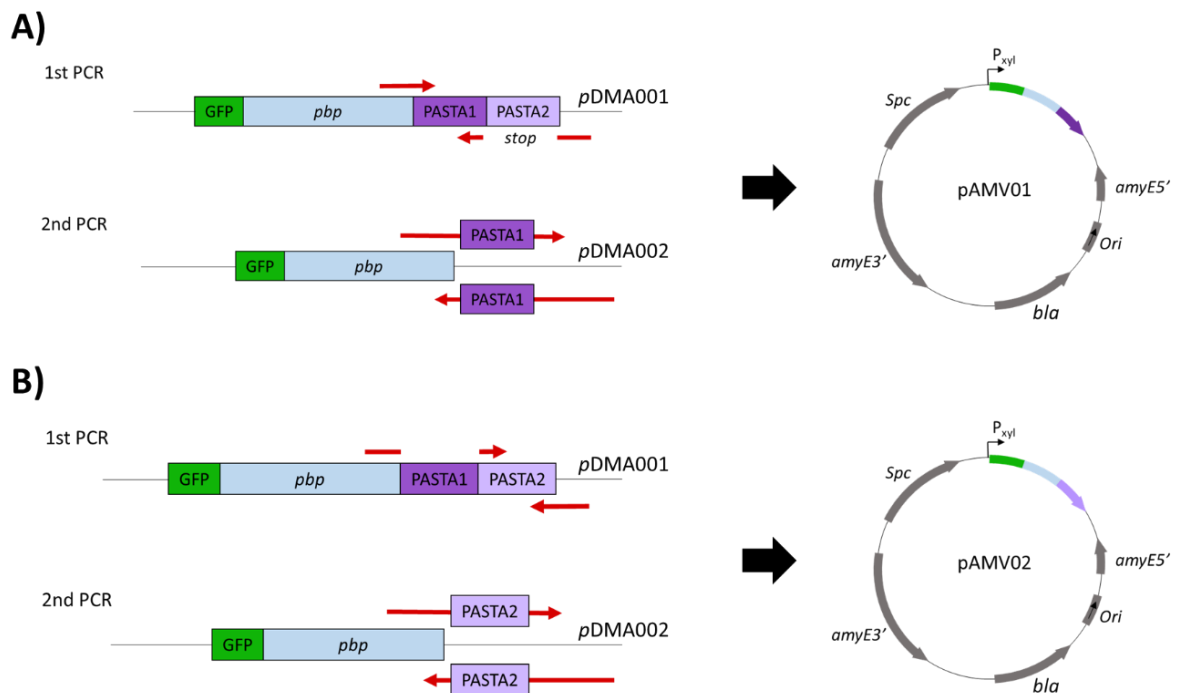


Figure 4. Scheme of molecular cloning protocol followed A) with primers amv01 and amv02 in order to obtain pAMV01 (deletion of PASTA2 domain) and B) with primers amv03 and amv04 for acquisition of pAMV02 (deletion of PASTA1 domain) using restriction free cloning.

3. Results

Deletion of PASTA domains has a negative effect on the DivIB-PBP2b interaction

Strains 4174 and 4175 had been previously obtained inserting GFP-PBP2b and GFP-PBP2b Δ PASTA, respectively, in GP2005, a strain that produces a flag-tagged version of DivIB under the control of its natural promoter, a kind gift from Jörg Stülke. All three strains were cultured until exponential phase. Membrane proteins were isolated according to the protocol explained in Materials and Methods. GFP-PBP2b variants were pulled down using anti-GFP nanobodies coupled to agarose beads. The presence of PBP2b mutants in the immunoprecipitate was visualised via Western blot using anti-GFP antibodies (IP; immunoprecipitation), while DivIB was observed using anti-FLAG antibodies (coIP; co-immunoprecipitation). Quantification of results was performed by analysing the amount of protein in the immunoblots with ImageJ. Results of four different replicates are presented in Figure 5. Input of the immunoblots corresponds to protein samples before incubation with the GFP-agarose beads. Flowthrough shows the amount of protein that was incubated with the beads but was not bound to them. Finally, IP and CoIP show the amount of PBP2b variants and DivIB pulled down with the beads, respectively. Figure 5A shows IP results. Binding of GFP-PBP2b and GFP-PBP2b Δ PASTA to the GFP-agarose beads worked, as PBP2b variants are clearly visible with the expected size: 106.02 KDa for PBP2b (79.12 KDa + 26.9 KDa from GFP) and 93.12 KDa for PBP2b Δ PASTA. Moreover, the claimed binding was efficient, as the amount of protein present in flowthrough of strains 4174 and 4175 is low. In figure 5B, coIP results are presented. DivIB was successfully co-immunoprecipitated, as bands with the corresponding size can be observed: 3 times flag-tag (1.012 KDa) + 30.02 KDa \approx 33.1 KDa. Incubation of immunoblots with anti-flag antibodies shows that pulling down efficiency of DivIB was low, as the amount of that protein present in flowthrough is higher than in the coIP, suggesting that the interaction between PBP2b and DivIB is not very strong. Unfortunately, control strain GP2005 showed a certain amount of protein in the coIP. In principle, this strain should not show any signal, as there is no protein fused to GFP that binds to DivIB and the agarose beads; thus, the emergence of that band must be due to a non-specific interaction. It could be an interaction between the protein and either the agarose bead or the GFP antibody coupled to it. The protocol used includes a pre-incubation of sample proteins with agarose beads (with no antibody), whereby non-specific interactions with the beads are already discarded; and a pre-incubation of beads with 1% (wt/vol) BSA, where that big protein interacts with the agarose and impedes the interaction of DivIB with it. Consequently, non-specific interactions observed in the coIP are most likely due to interactions of DivIB (or the flag-tag) with the GFP antibody. Those interactions might be still possible in strains 4174 and 4175 but are less favoured compared to the specific interaction of GFP- PBP2b with the GFP agarose beads.

The amount of PBP2b variants and DivIB pulled down was quantified with ImageJ. Despite the previous equilibration of protein concentration to 200ng for each coIP, the material in the immunoblot cannot be directly compared between strains as the method used determined amount of membrane proteins in sample, not only the concentration of the proteins of interest. In addition, experimental errors are present in all pipetting steps of this protocol. Consequently, the amount of protein added per strain is different as it can be perceived in Figure 5A for all inputs. Thus, the intensity of the coIP samples has been divided by their corresponding inputs and the resulting ratio has been compared between strains. Unfortunately, the non-specific binding seen in the control strain (GP2005) was variable among repetitions, so the standard deviation was remarkably high (Figure 5C). Results from the GP2005 strain could suggest that there is no interaction between DivIB and PBP2b when PASTA

domains are deleted as the mean of coIP/input values is higher for the control than for the Δ PASTA strain. However, results from D. Morales Ángeles⁵⁶ already demonstrated that there is still an interaction. The great variability of results together with the indication that there is no interaction between DivIB and PBP2b Δ PASTA led to the conclusion that GP2005 strain could not be used to obtain any information. In terms of strains 4174 and 4175, full length PBP2b showed a higher amount of DivIB pulled down than the mutant with no PASTA domains. That difference could be due to the fact that those regions are involved in the DivIB-PBP2b interaction. Results from coIP/input are visible in figure 5C and plotted in figure 5D.

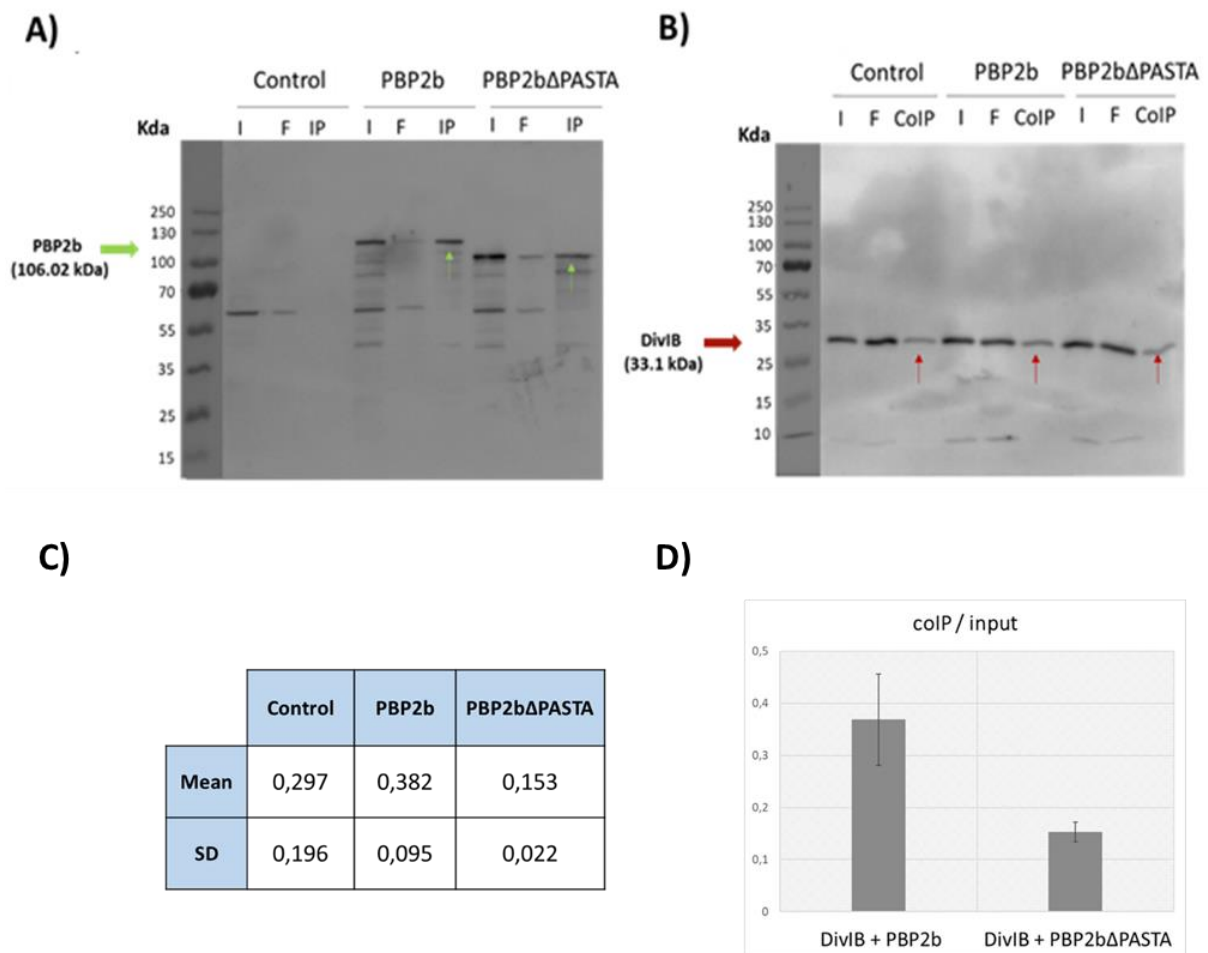


Figure 5. Results from co-immunoprecipitation assay with GFP beads. Control, PBP2b and PBP2b Δ PASTA stand for strains GP2005, 4174 and 4175, respectively. I: input; F: flowthrough; IP: immunoprecipitation; coIP: co-immunoprecipitation. Arrows point at the protein of interest. A) Results from incubation of immunoblots with anti-GFP antibodies demonstrate the production of PBP2b variants. B) Results from incubation of immunoblots with anti-flag antibodies show DivIB pulled down for all three strains as a consequence of a sum between DivIB-PBP2b interaction and non-specific interactions of the first protein with beads used. C) Table with results from quantification of co-immunoprecipitation bands of DivIB divided by the corresponding input from most promising immunoblots using ImageJ software. D) Schematic visualisation of values from (C), coIP/input of DivIB in strains 4174 and 4175 (from left to right). N = 5.

In view of the lack of a control for the experiment, a different approach was attempted. In this case, PVDF membranes were incubated with anti-GFP and anti-FLAG antibodies in order to visualise both proteins, PBP2b and DivIB, simultaneously. Subsequently, the ratio between the amount of PBP2b variant and DivIB pulled down was calculated. As can be seen already at first glance in Figure 6A, strain 4175 shows a lower amount of DivIB pulled down in comparison with strain 4174 with full length PBP2b, so the consistency of results is confirmed. Unfortunately, the values of intensities from the coIP

bands differed between blots, resulting in a quantification that was too variable to be used (Figure 6B, N=2). Notwithstanding, the difference between strains was seen in both methods and it is clear that the deletion of PASTA mutants had a negative effect on DivIB-PBP2b interaction.

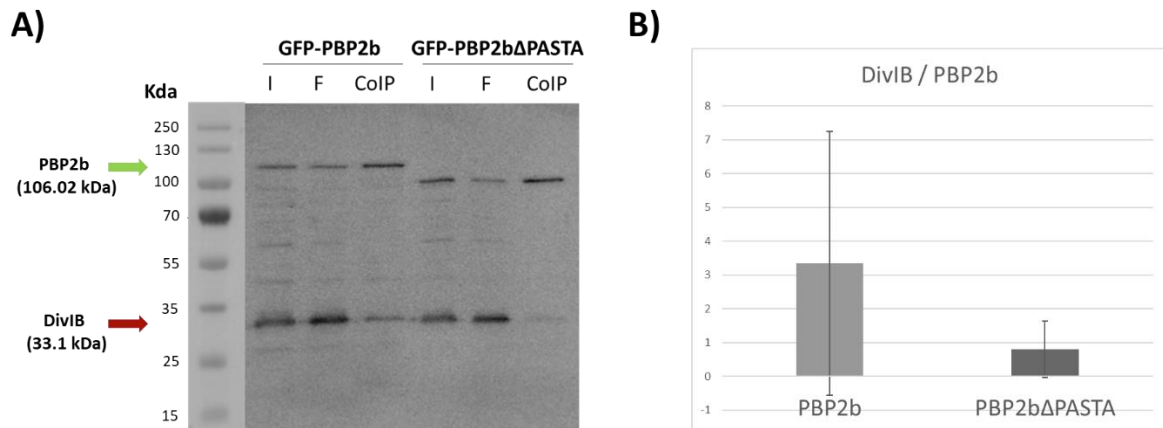


Figure 6. GFP-PBP2b and GFP-PBP2bΔPASTA stand for strains 4174 and 4175, respectively. **A)** PVDF membrane from immunoblotting incubated with anti-GFP and anti-flag antibodies showing a higher amount of DivIB pulled down when using full length PBP2b. **B)** Representation of DivIB coIP divided by PBP2b variant coIP. Results from two different duplicates together show a high variability between values after quantification with ImageJ.

Co-immunoprecipitation assays with flag-beads were attempted as well but turned out to be unsuccessful (Figure 7). Although DivIB could be observed for all three strains as expected, immunoblots incubated with anti-flag antibodies showed a significant amount of non-specific bands (Figure 7A). In the case of immunoblots with anti-flag antibodies, GP2005 had no band as that strain does not produce a GFP-PBP2b variant. However, neither GFP-PBP2b nor GFP-PBP2bΔPASTA from strains 4174 and 4175, respectively, were successfully pulled down, as it can be observed in Figure 7B. It is most likely that samples were lost in the washes as flowthrough does not show a considerable amount of protein compared to the input. Some optimization of the protocol could be performed in order to be able to visualise the protein. Interestingly, it can be seen again how, despite protein equilibration, input of strain 4175 shows a higher amount of protein than strain 4174 (Figure 7B), confirming the experimental error mentioned above.

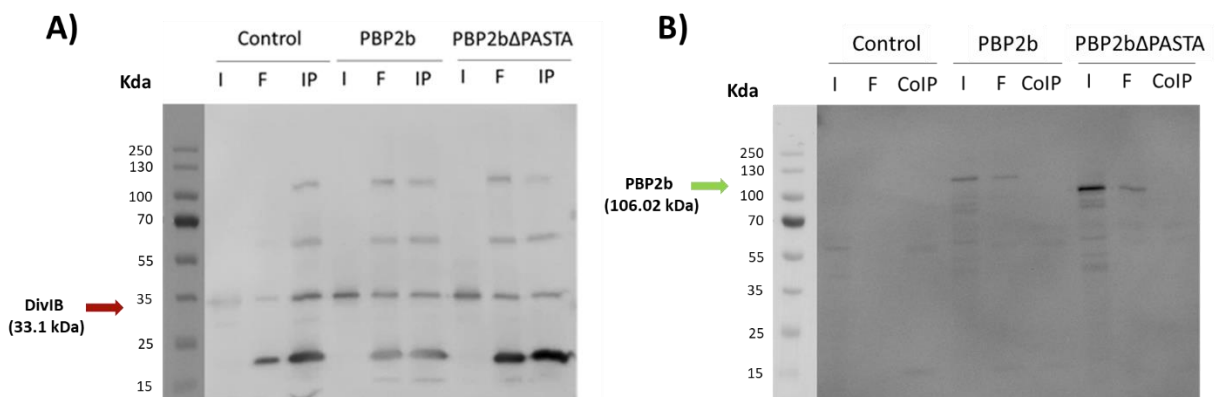


Figure 7. Results from co-immunoprecipitation assay with flag beads. Control, PBP2b and PBP2bΔPASTA stand for strains GP2005, 4174 and 4175, respectively. I: input; F: flowthrough; IP: immunoprecipitation; coIP: co-immunoprecipitation. **A)** Results from incubation of immunoblots with anti-flag antibodies produced non-specific interactions. **B)** Immunoblots incubated with anti-GFP antibodies did not show PBP2b pulled down.

PBP2b localisation at the division site is hindered in the absence of PASTA domains

D. Morales Angeles and colleagues already showed that, in the absence of PASTA domains, PBP2b is still recruited to the division site during cell division¹². Thus, PASTA domains are not essential for the interaction between PBP2b and DivIB. However, that claimed interaction is altered to a certain extent as seen in the co-immunoprecipitation results. Therefore, it was interesting to see whether the division site localisation was somehow impaired. In this experiment, strains used contain the native PBP2b under P_{spac} control, which means that wild-type protein was not expressed as long as IPTG was not included in the growth medium, and thus could not influence results. Exponentially growing cells from strains 4132 and 4133 were scored for the presence of the GFP-PBP2b variant at the division site. $58.78 \pm 4.86\%$ cells ($n = 609$) with full length PBP2b showed protein localised at the division site in contrast to $37.79 \pm 0.95\%$ cells ($n = 606$) without the PASTA domains. Those results were analysed via a Chi-square test and the null hypothesis was rejected with a p -value ≤ 0.01 . That means, there is a significant difference of recruitment efficiency when PBP2b does not contain the two PASTA domains. This could be explained by the fact that interaction between PBP2b and other proteins from the late divisome such as DivIB is likely to be hampered, so recruitment of PBP2b is impeded.

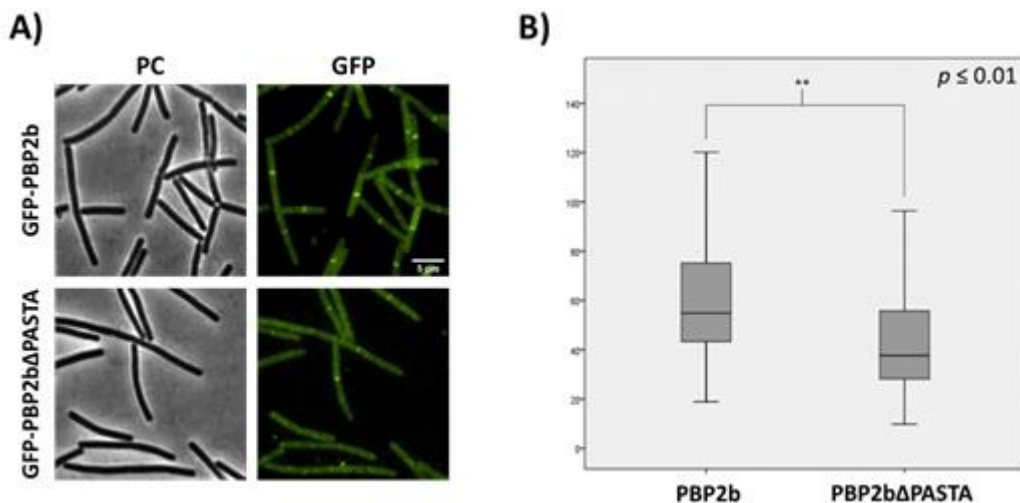


Figure 8. Results from intensity measurements under the microscope. PC and GFP correspond to phase contrast and fluorescent light. GFP-PBP2b and GFP-PBP2b Δ PASTA stand for strains 4132 and 4133, respectively. A) Visualisation under the microscope. B) Intensity measurements represented in boxplots.

Another characteristic observed was the difference of intensity at the division site of cells where PBP2b variants were localised. At first glance it seemed that cells with full length protein show a more intense fluorescent septum. Relative intensity was measured as the difference between fluorescent signal at the division site and background at the sides of the septum (Figure 3) and quantified in arbitrary units. Results represented in boxplots in Figure 8 show the difference between strains 4132 and 4133. The null hypothesis is rejected when p -value ≤ 0.01 . However, those data can give an insight or provide with some additional proof but cannot be taken completely into consideration as the production of both proteins (full length and Δ PASTA) has not been compared. Although growth and induction were performed under the same conditions and growth state of the cells was similar before microscopic observation, it could be that PBP2b Δ PASTA production is decreased, which would also explain the decrease in intensity.

Cloning of PASTA constructs

Constructs with one single PASTA domain could provide deeper information about how DivIB-PBP2b interaction is mediated and which residues are involved. In order to get those mutants, pDMA001 and pDMA002 were successfully transformed in *E. coli* by heat-shock for production and isolation. Subsequently, pDMA001 was amplified in parallel with i) amv01 and amv02 to obtain a PBP2b-PASTA1 mutant and ii) amv03 and amv04 to obtain a PBP2b-PASTA2 mutant. For that PCR, some protocol optimisations were performed in comparison with the standard one proposed⁶⁴ (Table 2). Products obtained in that PCR reaction for both constructs can be seen in Figure 9, with the correct size according to predictions from <http://www.rf-cloning.org/> (accessed July 5th, 2019). A second PCR was planned using pDMA002 as a template and products of the first PCR mentioned as mega-primers in order to insert the PASTA domains in a plasmid with GFP for future co-immunoprecipitation assays and observation under the microscope. However, the second PCR did not give any product; therefore, the completion of the cloning plan and subsequent transformation in *B. subtilis* for further work was not possible.

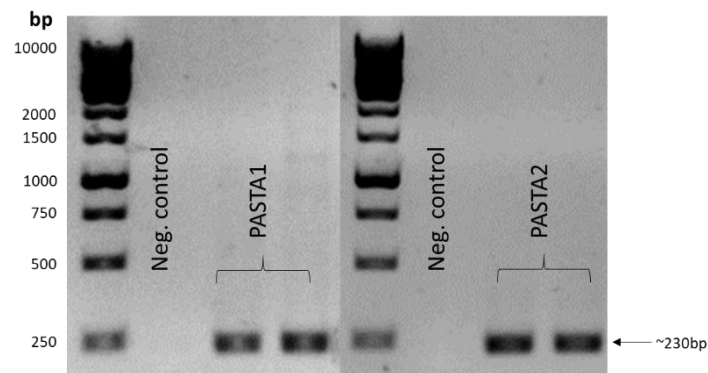


Figure 9. Results from 1st PCR of restriction free cloning. Mega-primer for PASTA1 (no PASTA2 domain) and PASTA2 (no PASTA 1 domain) are successfully obtained as there is no band in the negative control, which means there is no primer dimerization.

4. Discussion and conclusions

Protein-protein interactions are a subject of interest as they provide information about molecular networks, functions and mechanisms of how physiological processes are mediated. Due to their importance, methodologies such as bacterial two hybrid assays and co-immunoprecipitation analysis have long been used. For example, the interaction between PBP2b and DivIB was first seen by bacterial two hybrid assay³⁶, while connections between other division proteins were better understood thanks to co-immunoprecipitation experiments in *B. subtilis*⁵⁷. Other PBP relationships have been studied in different species such as *S. pneumoniae* by performing crosslinking-coIP experiments⁶⁶. In eukaryotes, those methods have also been utilised to acquire a better insight of protein-protein interactions. A novel interacting mitochondrial protein has been identified in human kidney cells via coIP coupled to mass spectrometry⁶⁷.

In this work, co-immunoprecipitation assays have been used to explore the influence of PASTA domains with DivIB. As mentioned above, results from the control strain showed that there is some non-specific interaction between DivIB and the beads used. That interaction is likely to happen between the GFP antibody coupled to beads used and DivIB, as the protocol followed includes the pre-clearing of protein samples and blocking of beads with BSA, steps explained in previous sections. Most likely, that non-specific interaction is favoured in the absence of either mutant of PBP2b. It is possible

that this interaction is still present in strains 4174 and 4175, although hindered by the specificity between GFP-PBP2b variants and GFP antibodies of the agarose beads. Consequently, in order to improve the setup of this experiment, a more suitable control strain that provides information about that background is required. For that purpose, an empty plasmid with P_{xyl}-GFP inserted in GP2005 could be a good candidate.

In the case of strains 4174 and 4175, both showed some interaction between the corresponding variant of PBP2b and DivIB. However, coIPs showed a decreased interaction between PBP2b Δ PASTA and DivIB in comparison to the full length protein, as the amount of DivIB co-immunoprecipitated was substantially higher. Interestingly, it should be taken into account that strains used in co-immunoprecipitation assays still produce a wild-type PBP2b protein under its natural promoter. Consequently, DivIB-3xflag might interact with the wild-type protein. On the one hand, that could be a possible explanation for the low efficiency of the coIP in comparison with the IP (Figure 5 A and B). Although that could be explained by a weak interaction or the fact that DivIB is under expression of its natural promoter, while PBP2b is overexpressed. On the other hand, it could be that in the presence of both PBP2b full length (wild-type) and GFP-PBP2b Δ PASTA in strain 4175, interaction with the full length protein is favoured, which in any case would indicate that the presence of PASTA domains stabilises that claimed interaction. It has been previously reported that PBP2b PASTA domains are not essential for the DivIB-PBP2b interaction. Bacterial two hybrid screening from D. Morales Angeles and colleagues confirmed that there is still some interaction between those two proteins when PASTA domains are deleted (Figure 10)⁵⁶. Nevertheless, a difference between full length protein and a truncated version without the two PASTA domains was seen when measuring bacterial two hybrid β -galactosidase activity (Figure 10B), in agreement with co-immunoprecipitation results from this work. Altogether suggest that, although not exclusively, PASTA domains are involved in DivIB-PBP2b interaction and the deletion of those regions has a negative effect on it.

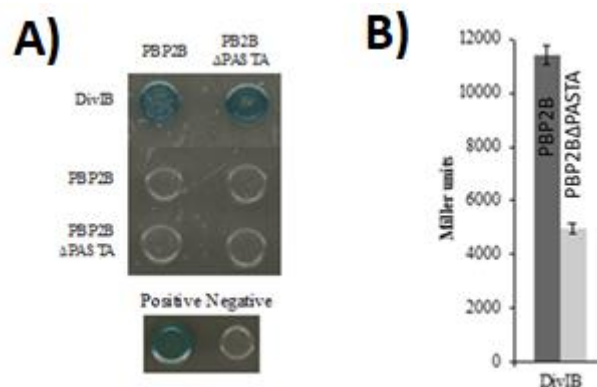


Figure 10. Adapted from D. Morales Angeles, PhD thesis, 2018⁵⁶. Results show that there is a hindered interaction between DivIB and PBP2b when PASTA domains are deleted. A) Bacterial two hybrid Screening assay on plates containing X-Gal. B) Bacterial two hybrid β -galactosidase activity measurement.

In terms of the reverse experiment, where DivIB flag-tagged was immunoprecipitated, there were many non-specific interactions both in the flowthrough and IP. The presence of those non-specific binding proteins can be corrected incubating membrane proteins with agarose beads with no antibody, as for GFP-beads. Unfortunately, no immunoblot showed any of the PBP2b variants pulled down. Based on results, PBP2b is produced, as it is visible in the input for both strains 4174 and 4175. Moreover, flowthrough does not show a great amount of protein; thus, it could be that PBP2b did bind to DivIB but was lost during washing steps. Firstly, in order to confirm that the problem lies on washing,

washes should be collected and visualised in a gel. If that was the case, some steps of the protocol followed could be optimised. According to manufacturers, incubation of the protein sample is continued by a set of washes. One improvement could be to decrease the amount of washes done for that protocol; another option would be to wash the beads but not incubate with wash buffer, as done for GFP-beads.

Microscopy experiments from D. Morales Angeles and peers have proven that PBP2b is still recruited to the division site in the absence of the PASTA domains⁵⁶, one more proof that those C-terminus regions are not indispensable for DivIB-PBP2b interaction. However, in this work it has been observed that cells without PBP2b PASTA domains exhibit a significantly impaired localisation at the division site compared to full length protein cells. In combination with co-immunoprecipitation results, it seems that PASTA domains are involved in DivIB-PBP2b interaction and might strengthen it, increasing the efficiency of PBP2b recruitment to the division site during cell wall biosynthesis. Regarding intensity measurements, a significant difference has been observed between strains. Nevertheless, protein production of both PBP2b variants has not been compared; thus, it cannot be stated that those results are relevant. In order to acquire more accurate results, a different quantification of the pictures taken from the microscope should be performed: fluorescence of entire cells should be measured. In that case, not only the difference between division site and cytosolic fluorescence would be taken into account, but also the total amount of fluorescence produced by PBP2b present in the cytosol.

It has been reported that Δ PASTA strains of *B. subtilis* have a cell length defect and are heat sensitive⁵⁶. However, thermal stability of PBP2b was not compromised in the absence of the PASTA domains. Similarly, a Δ DivIB strain shows sensitivity to high temperatures and an analogous elongated phenotype. Increase of cell length suggests a division defect. It could be that at high temperatures the proteins individually do not suffer any alteration but the interaction between them does, which would give a reasonable explanation why stability of both proteins is not jeopardized. It has been seen that mutations at the C-terminal of DivIB⁶⁸ confer temperature sensitivity to cells, which is, based on computational model, the region suggested to be involved in the interaction with PBP2b³⁸. Therefore, weak interactions between the C-terminus of DivIB and the transpeptidase domain of PBP2b may occur, such as hydrogen bonds or salt bridges, which would be, theoretically, stabilized by cause of steadier or higher number of interactions with the two PASTA domains of PBP2b. In that way, heat sensitivity of Δ DivIB and Δ PASTA strains could be explained, while wild-type cells would show a normal phenotype. Interactions between PASTA domains and DivIB should not be necessary different. Hydrogen bonds, for instance, have been seen to be thermal sensitive⁶⁹; however, it has been reported that a considerable amount of hydrogen bonds can increase the thermal stability of a protein⁷⁰. Therefore, interactions with PASTA domains could still have the same chemical nature but an increase in the number of bonds would still favour the stabilisation of the protein-protein interaction. Elucidation of the type of interactions taking place between PBP2b and DivIB during cell wall biosynthesis requires further research. Although there are still some questions remaining, it can be stated with certainty that PASTA domains are involved in the DivIB-PBP2b interaction.

5. Further work

There are some aspects of the protocols used in this work that could be improved in terms of the setup of the experiments. The possibility of inserting a plasmid containing GFP in strain GP2005 has been already mentioned in the previous section. Plasmid pSG1729 from P. J. Lewis and A. L. Marston⁷¹ should be a good alternative as plasmids inserted in 4174 and 4175 (pDMA001 and pDMA002) were originally cloned using it as a template. With a more suitable control, background produced by non-specific binding proteins could be taken into account in quantification of immunoblots.

In terms of co-immunoprecipitation assays with flag-tagged beads, modifications of the protocol regarding washing steps commented in Discussion and Conclusions could be attempted. If PBP2b is not successfully pulled down, there is a wide range of changes that can be assayed, such as elongation of incubation time or modification of buffers composition, among others.

In respect of relative intensity measurements, the total amount of fluorescence produced by PBP2b and PBP2b Δ PASTA both in the cytosol and at the division site should be considered for a proper quantification, as described above.

It has been hypothesised that DivIB-PBP2b interaction might be heat sensitive. Surface plasmon resonance (OpenSPR, Nicoyalife) is a technique that offers a wide range of opportunities as it provides information about interaction and kinetics at different temperatures; thus, it would be interesting to test the interaction between those late divisome proteins and see how increase of temperature affects.

Regarding PASTA1 and PASTA2 constructs, more time is required to improve the second PCR protocol and acquire a positive result that can be transformed in *B. subtilis*. Once transformants have been successfully achieved, characterisation of their phenotypes under the microscope and exploration of the interaction between those mutants and DivIB should be performed. PASTA domains involvement in DivIB-PBP2b interaction has been demonstrated. However, the transpeptidase domain of the latter protein is likely to be involved as well. A library of mutants from the C-terminal of that domain could give more information about the residues involved. Mutation should be preferable as deletions could impede the interaction due to a change in the whole structure, leading to misconceptions.

Finally, the acquisition of a high resolution structure of both DivIB and PBP2b by electron microscopy or crystallisation, for instance, would give the fundamental information to elucidate and understand how that interaction is mediated during peptidoglycan synthesis.

6. References

1. INTERNATIONAL COMMITTEE ON SYSTEMATIC BACTERIOLOGY SUBCOMMITTEE ON THE TAXONOMY OF MOLLICUTES. Revised Minimum Standards for Description of New Species of the Class MoZZicutes (Division Tenericutes). 605–612 (1995).
2. Navarre, W. W. & Schneewind, O. Surface Proteins of Gram-Positive Bacteria and Mechanisms of Their Targeting to the Cell Wall Envelope. **63**, 174–229 (1999).
3. Dramsi, S., Magnet, S., Davison, S. & Arthur, M. Covalent attachment of proteins to peptidoglycan. *FEMS Microbiol. Rev.* **32**, 307–320 (2008).

4. Scheffers, D. & Pinho, M. Bacterial Cell Wall Synthesis: New Insights from Localization Studies. *Am. Soc. Microbiol.* **69**, 585–607 (2005).
5. Sarkar, P., Yarlagadda, V., Ghosh, C. & Haldar, J. A review on cell wall synthesis inhibitors with an emphasis on glycopeptide antibiotics. *Medchemcomm* **8**, 516–533 (2017).
6. Matias, V. R. F. & Beveridge, T. J. Cryo-electron microscopy reveals native polymeric cell wall structure in *Bacillus subtilis* 168 and the existence of a periplasmic space. *Mol. Microbiol.* **56**, 240–251 (2005).
7. Hayhurst, E. J., Kailas, L., Hobbs, J. K. & Foster, S. J. Cell wall peptidoglycan architecture in *Bacillus subtilis*. *Proc. Natl. Acad. Sci.* **105**, 14603–14608 (2008).
8. Neuhaus, F. C. & Baddiley, J. A Continuum of Anionic Charge: Structures and Functions of D-Alanyl-Teichoic Acids in Gram-Positive Bacteria. *Microbiology* **67**, 686–723 (2003).
9. Bhavsar, A. P., Erdman, L. K., Schertzer, J. W. & Brown, E. D. Teichoic Acid Is an Essential Polymer in *Bacillus subtilis* That Is Functionally Distinct from Teichuronic Acid. *J. Bacteriol.* **186**, 7865–7873 (2004).
10. Van Heijenoort, J. Recent advances in the formation of the bacterial peptidoglycan monomer unit. *Nat. Prod. Rep.* **18**, 503–519 (2001).
11. Vollmer, W., Blanot, D. & De Pedro, M. A. Peptidoglycan structure and architecture. *FEMS Microbiol. Rev.* **32**, 149–167 (2008).
12. D. Morales Angeles, Y. Liu, A. M. Hartman, M. Borisova, A. de Sousa Borges, N. de Kok, K. Beilharz, J. W. V. & C. Mayer, A. K. H. H. and D. J. S. Pentapeptide-rich peptidoglycan at the *Bacillus subtilis* cell-division site. **104**, 319–333 (2017).
13. Bouhss, A., Trunkfield, A. E., Bugg, T. D. H. & Mengin-Lecreulx, D. The biosynthesis of peptidoglycan lipid-linked intermediates. *FEMS Microbiol. Rev.* **32**, 208–233 (2008).
14. Barreteau, H. *et al.* Cytoplasmic steps of peptidoglycan biosynthesis. *FEMS Microbiol. Rev.* **32**, 168–207 (2008).
15. Manat, G. *et al.* Deciphering the Metabolism of Undecaprenyl-Phosphate: The Bacterial Cell-Wall Unit Carrier at the Membrane Frontier. *Microb. Drug Resist.* **20**, 199–214 (2014).
16. Scheffers, D. J. & Tol, M. B. LipidIII: Just Another Brick in the Wall? *PLoS Pathog.* **11**, 1–12 (2015).
17. Teo, A. C. & Roper, D. I. Core Steps of Membrane-Bound Peptidoglycan Biosynthesis: Recent Advances, Insight and Opportunities. *Antibiotics* **4**, 495–520 (2015).
18. Meeske, A. J. *et al.* SEDS proteins are a widespread family of bacterial cell wall polymerases. *Nat. Rev Drug Discov.* **5**, 1–26 (2017).
19. Emami, K. *et al.* RodA as the missing glycosyltransferase in *Bacillus subtilis* and antibiotic discovery for the peptidoglycan polymerase pathway. *Nat. Microbiol.* **2**, 16253 (2017).
20. Borisova, M. *et al.* Peptidoglycan Recycling in Gram-Positive Bacteria Is Crucial for Survival in Stationary Phase. *MBio* **7**, 1–10 (2016).
21. Litzinger, S. *et al.* Muropeptide rescue in *Bacillus subtilis* involves sequential hydrolysis by β -N-acetylglucosaminidase and N-acetylmuramyl-L-alanine amidase. *J. Bacteriol.* **192**, 3132–3143 (2010).
22. Wilmes, M., Cammue, B. P. A. & Sahl, H. G. Antibiotic Activities of Host Defense Peptides :

- More to it than Lipid Bilayer Perturbation. *R. Soc. Chem.* (2011). doi:10.1039/c1np00022e
23. Macheboeuf, P., Contreras-Martel, C., Job, V., Dideberg, O. & Dessen, A. Penicillin binding proteins: Key players in bacterial cell cycle and drug resistance processes. *FEMS Microbiol. Rev.* **30**, 673–691 (2006).
 24. Knowles, J. R. Penicillin Resistance: The Chemistry of β -Lactamase Inhibition. *Acc. Chem. Res.* **18**, 97–104 (1985).
 25. Goffin, C. & Ghuysen, J. M. Multimodular penicillin-binding proteins: an enigmatic family of orthologs and paralogs. *Microbiol. Mol. Biol. Rev.* **62**, 1079–93 (1998).
 26. Koch, A. L. Penicillin binding proteins, β -lactams, and lactamases: Offensives, attacks, and defensive countermeasures. *Crit. Rev. Microbiol.* **26**, 205–220 (2000).
 27. Sauvage, E., Kerff, F., Terrak, M., Ayala, J. A. & Charlier, P. The penicillin-binding proteins: Structure and role in peptidoglycan biosynthesis. *FEMS Microbiol. Rev.* **32**, 234–258 (2008).
 28. Strominger, P. J. L. and Ja. L. Biosynthesis of the Peptidoglycan of Bacterial Cell Walls. XVI. The reversible fixation of radioactive penicillin G to the D-Alanine carboxylpeptidase of *Bacillus subtilis*. *J. Biol. Chem.* **245**, 3660–3666 (1969).
 29. Scheffers, D. J. Dynamic localization of penicillin-binding proteins during spore development in *Bacillus subtilis*. *Microbiology* **151**, 999–1012 (2005).
 30. Claessen, D. *et al.* Control of the cell elongation-division cycle by shuttling of PBP1 protein in *Bacillus subtilis*. *Mol. Microbiol.* **68**, 1029–1046 (2008).
 31. Yanouri, A., Daniel, R. A., Errington, J. & Buchanan, C. E. Cloning and sequencing of the cell division gene *pbpB*, which encodes penicillin-binding protein 2B in *Bacillus subtilis*. *J. Bacteriol.* **175**, 7604–16 (1993).
 32. Daniel, R. A., Harry, E. J. & Errington, J. Role of penicillin-binding protein PBP 2B in assembly and functioning of the division machinery of *Bacillus subtilis*. *Mol. Microbiol.* **35**, 299–311 (2000).
 33. Sassine, J. *et al.* Functional redundancy of division specific penicillin-binding proteins in *Bacillus subtilis*. *Mol. Microbiol.* **106**, 304–318 (2017).
 34. Gamba, P., Veening, J. W., Saunders, N. J., Hamoen, L. W. & Daniel, R. A. Two-step assembly dynamics of the *Bacillus subtilis* divisome. *J. Bacteriol.* **191**, 4186–4194 (2009).
 35. Scheffers, D. J., Jones, L. J. F. & Errington, J. Several distinct localization patterns for penicillin-binding proteins in *Bacillus subtilis*. *Mol. Microbiol.* **51**, 749–764 (2004).
 36. Daniel, R. A., Noirot, P. & Errington, J. Multiple Interactions between the Transmembrane Division Proteins of *Bacillus subtilis* and the Role of FtsL Instability in Divisome Assembly. *Am. Soc. Microbiol.* **188**, 7396–7404 (2006).
 37. Robichon, C., King, G. F., Goehring, N. W. & Beckwith, J. Artificial Septal Targeting of *Bacillus subtilis* Cell Division Proteins in *Escherichia coli* : an Interspecies Approach to the Study of Protein-Protein Interactions in Multiprotein Complexes. *J. Bacteriol.* **190**, 6048–6059 (2008).
 38. Rowland, S. L. *et al.* Evidence from Artificial Septal Targeting and Site-Directed Mutagenesis that Residues in the Extracytoplasmic \square Domain of DivIB Mediate Its Interaction with the Divisomal Transpeptidase PBP 2B. *Am. Soc. Microbiol.* **192**, 6116–6125 (2010).
 39. Ruggiero, A., De Simone, P., Smaldone, G., Squeglia, F. & Berisio, R. Bacterial Cell Division

- Regulation by Ser/Thr Kinases: A Structural Perspective. *Curr. Protein Pept. Sci.* **13**, 756–766 (2017).
40. Dworkin, J. Ser/Thr phosphorylation as a regulatory mechanism in bacteria. *Curr. Opin. Microbiol.* **24**, 47–52 (2015).
 41. Pares, S., Mouz, N., Pétillet, Y., Hakenbeck, R. & Dideberg, O. X-ray structure of *Streptococcus pneumoniae* PBP2x, a primary penicillin target enzyme. *Nat. Publ. Gr.* **3**, 284–289 (1996).
 42. Yeats, C., Finn, R. D. & Bateman, A. The PASTA domain: A β -lactam-binding domain. *Trends Biochem. Sci.* **27**, 438–440 (2002).
 43. Calvanese, L., Falcigno, L., Squeglia, F., Berisio, R. & D’Auria, G. PASTA sequence composition is a predictive tool for protein class identification. *Amino Acids* **50**, 1441–1450 (2018).
 44. Squeglia, F. *et al.* Chemical basis of peptidoglycan discrimination by PrkC, a key kinase involved in bacterial resuscitation from dormancy. *J. Am. Chem. Soc.* **133**, 20676–20679 (2011).
 45. Shah, I. M., Laaberki, M.-H., Popham, D. L. & Dworkin, J. A Eukaryotic-like Ser/Thr Kinase Signals Bacteria to Exit Dormancy in Response to Peptidoglycan Fragments. *NIH Public Access* **23**, 1–7 (2008).
 46. Pompeo, F., Byrne, D., Mengin-Lecreulx, D. & Galinier, A. Dual regulation of activity and intracellular localization of the PASTA kinase PrkC during *Bacillus subtilis* growth. *Sci. Rep.* **8**, 1–12 (2018).
 47. Daniel, R. A., Drake, S., Buchanan, C. E., Scholle, R. & Errington, J. The *Bacillus subtilis* spoVD gene encodes a mother-cell-specific penicillin-binding protein required for spore morphogenesis. *J. Mol. Biol.* **235**, 209–220 (1994).
 48. Bukowska-Faniband, E. & Hederstedt, L. The PASTA domain of penicillin-binding protein SpoVD is dispensable for endospore cortex peptidoglycan assembly in *Bacillus subtilis*. *Microbiol. (United Kingdom)* **161**, 330–340 (2015).
 49. Sidarta, M., Li, D., Hederstedt, L. & Bukowska-Faniband, E. Forespore targeting of SpoVD in *Bacillus subtilis* is mediated by the N-terminal part of the protein. *J. Bacteriol.* **200**, 1–14 (2018).
 50. Mir, M. *et al.* The extracytoplasmic domain of the mycobacterium tuberculosis ser/thr kinase PknB binds specific muropeptides and is required for PknB localization. *PLoS Pathog.* **7**, (2011).
 51. Turapov, O. *et al.* The external PASTA domain of the essential serine/threonine protein kinase PknB regulates mycobacterial growth. *Open Biol.* **5**, (2015).
 52. Paracuellos, P. *et al.* The Extended Conformation of the 2.9-Å Crystal Structure of the Three-PASTA Domain of a Ser/Thr Kinase from the Human Pathogen *Staphylococcus aureus*. *J. Mol. Biol.* **404**, 847–858 (2010).
 53. Maestro, B. *et al.* Recognition of peptidoglycan and β -lactam antibiotics by the extracellular domain of the Ser/Thr protein kinase StkP from *Streptococcus pneumoniae*. *FEBS Lett.* **585**, 357–363 (2011).
 54. Beilharz, K. *et al.* Control of cell division in *Streptococcus pneumoniae* by the conserved Ser/Thr protein kinase StkP. *Proc. Natl. Acad. Sci.* **109**, E905–E913 (2012).
 55. Calvanese, L., Falcigno, L., Squeglia, F., D’Auria, G. & Berisio, R. Structural and dynamic

- features of PASTA domains with different functional roles. *J. Biomol. Struct. Dyn.* **35**, 2293–2300 (2016).
56. Angeles, D. M. LET OP! Cell wall under construction. Untangling *Bacillus subtilis* cell wall synthesis. (Rijksuniversiteit Groningen, 2018).
 57. D.J. Scheffers, C. Robichon, G. J. Haan, T. den & Blaauwen, G. Koningstein, E. van Bloois, J. B. and J. L. Contribution of the FtsQ Transmembrane Segment to Localization to the Cell Division Site. *Am. Soc. Microbiol.* **189**, 7273–7280 (2007).
 58. Switzer, C. Sensitive Silver Stain for Detecting Proteins Peptides in Polyacrylamide Gels. **237**, 231–237 (1979).
 59. Schindelin, J. *et al.* Fiji - an Open Source platform for biological image analysis. *Nat. Methods* **9**, (2019).
 60. Mchugh, M. L. The Chi-square test of independence. *Lessons Biostat.* **23**, 143–149 (2013).
 61. Syvertsson, S., Vischer, N. O. E., Gao, Y. & Hamoen, L. W. When Phase Contrast Fails : ChainTracer and NucTracer , Two ImageJ Methods for Semi- Automated Single Cell Analysis Using Membrane or DNA Staining. 1–11 (2016). doi:10.1371/journal.pone.0151267
 62. Jankowski, K. R. B. *et al.* The t -test : An Influential Inferential Tool in Chaplaincy and Other Healthcare Research. *J. Health Care Chaplain.* **24**, 30–39 (2018).
 63. Green, R. & Rogers, E. J. Chemical Transformation of *E. coli*. *Natl. Inst. Heal.* 1–4 (2013). doi:10.1016/B978-0-12-418687-3.00028-8.
 64. Bond, S. R. & Naus, C. C. RF-Cloning.org : an online tool for the design of restriction-free cloning projects. *Nucleic Acids Res.* **40**, 209–213 (2012).
 65. Koontz, L. Agarose Gel Electrophoresis. in *Methods in Enzymology* **529**, 35–45 (Elsevier Inc., 2013).
 66. Rued, B. E. *et al.* Suppression and synthetic-lethal genetic relationships of Δ gpsB mutations indicate that GpsB mediates protein phosphorylation and penicillin-binding protein interactions in *Streptococcus pneumoniae* D39. *Mol. Microbiol.* **103**, 931–957 (2017).
 67. Chen, R. *et al.* Identification of a novel mitochondrial interacting protein of C1QBP using subcellular fractionation coupled with CoIP-MS. *Anal. Bioanal. Chem.* **408**, 1557–1564 (2016).
 68. Harry, E. J., Stewart, B. J. & Wake, R. G. Characterization of mutations in divIB of *Bacillus subtilis* and cellular localization of the DivIB protein. *Mol. Microbiol.* **7**, 611–621 (1993).
 69. Dougherty, R. C. Temperature and pressure dependence of hydrogen bond strength: A perturbation molecular orbital approach. *J. Chem. Phys.* **109**, 7372–7378 (1998).
 70. Vogt, G., Woell, S. & Argos, P. Protein thermal stability, hydrogen bonds, and ion pairs. *J. Mol. Biol.* **269**, 631–643 (1997).
 71. Lewis, P. J. & Marston, A. L. GFP vectors for controlled expression and dual labelling of protein fusions in *Bacillus subtilis*. *Gene* **227**, 101–109 (1999).